It follows from (16) that in the case when the values of the accommodation coefficients γ_1 and γ_2 are close ($\gamma_1 \approx \gamma_2$) the equation obtained in [5] for the velocity U_p in a monatomic gas can be used to estimate the velocity of particle motion in a polyatomic gas. The error committed in doing this does not exceed 5%, as the above calculations showed.

NOTATION

n, number of gas molecules per unit volume; **v**, m, velocity and mass of a molecule; T, gas temperature at the position of the particle; E_i, internal energy of a molecule in the i-th quantum state; U_p, velocity of the given point of the particle's surface; $f_i^{\mp}$, distribution functions of incident (—) and reflected molecules; δ, coefficient of accommodation of tangential momentum; γ_1 and γ_2, energy accommodation coefficients for translational and internal energies of a molecule; q(r), density of heat sources; $\varkappa$, coefficient of thermal conductivity of particle material; T_{w0}, average temperature of reflected molecules; k, Boltzmann constant; **N**, **E**, flux densities of molecules and energy; **F**, **L**, force and force moment acting on a particle.

LITERATURE CITED

1. O. Preining, "Photophoresis," in: Aerosol Science, C. N. Davies (ed.), Academic Press, New York (1966).
2. Yu. I. Yalamov, V. B. Kutukov, and E. R. Shchukin, "Theory of motion of a small aerosol particle in an optical radiation field," Inzh.-Fiz. Zh., 30, 996-1002 (1976).
3. S. L. Gorelov, "Thermophoresis and photophoresis in a rarefied gas," Izv. Akad. Nauk SSSR, Mekh. Zhidk. Gaza, No. 5, 178-182 (1976).
4. M. N. Kogan, Rarefied Gas Dynamics, Plenum Publ. (1969).
5. M. G. Markov and E. R. Shchukin, "On the motion of small, volatile, aerosol particles in gas mixtures which are inhomogeneous in temperature and concentration," Izv. Vyssh. Uchebn. Zaved., Fiz., No. 2, 123 (1980); Dep. No. 4138-79, Vses. Inst. Nauchn. Tekh. Inform.

EFFECT OF A CORONA DISCHARGE FIELD ON EVAPORATION OF LIQUIDS FROM CAPILLARIES

I. N. Karpovich, N. V. Churaev, and M. S. Panchenko

UDC 536.423:537.212

Results of a study of the effect of a corona discharge field on evaporation of water and aqueous KCl solutions from quartz capillaries 2-30 μm in radius are presented.

It has been experimentally shown [1, 2] that the electric field of a corona discharge can have a significant effect on the mass-transfer properties of capillary—porous systems. To clarify the mechanism underlying this effect, it is of interest to study the effect of such a discharge on evaporation and motion of liquids in individual capillaries, which, as is well known, can serve as the simplest model of pores.

Measurements were made of the relative evaporation rate of pure water and aqueous KCl solutions from quartz capillaries 2-30 μm in radius in air at atmospheric pressure in a corona discharge field and with the field absent. Evaporation took place within the volume of a thermally stabilized chamber, in which a constant relative humidity φ was maintained by a saturated salt solution. The evaporation rate was determined from the displacement of the liquid meniscus x, which was determined by a KM-6 cathetometer as a function of time τ. The experimental equipment used, and the conditions under which experiments were performed

Institute of Physical Chemistry, Academy of Sciences of the USSR, Moscow. Ukrainian Institute of Hydrology, Rovno. D. Z. Manul'skii Roven State Pedagogic Institute.

Translated from Inzhenerno-Fizicheskii Zhurnal, Vol. 41, No. 6, pp. 1049-1056, December, 1981. Original article submitted September 9, 1980.

0022-0841/81/4106-1333$07.50

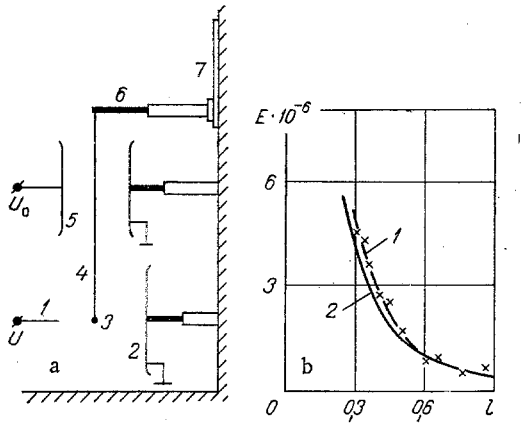

Fig. 1

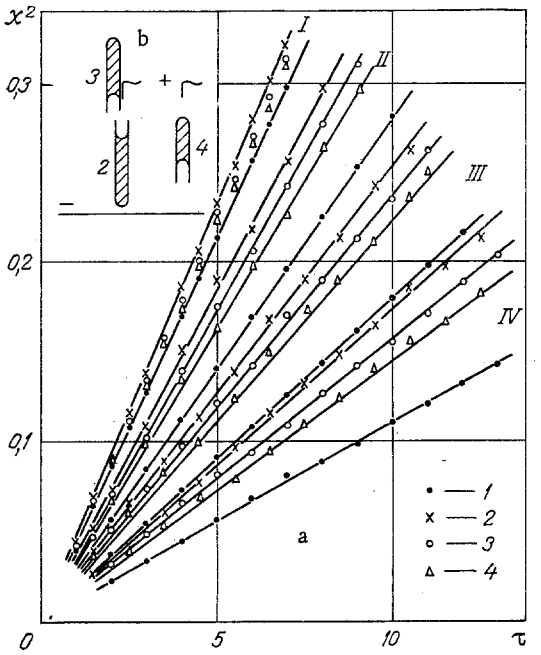

Fig. 2

Fig. 1. System for measurement of corona discharge field intensity with needle-plane electrode system (a); experimental (1) and calculated (2) field intensity distributions in evaporation zone (b). E, V/m; l, cm.

Fig. 2. Function $x^2(\tau)$ for water evaporation from quartz capillaries into air at 297°K (a) ($r = 16.8$ μm, $\varphi = 0$ (curve 1); $r = 5.5$ μm, $\varphi = 0.34$ (II); $r = 12.2$ μm, $\varphi = 0.58$ (III); $r = 19.6$ μm, $\varphi = 0.75$ (IV): 1) without field; 2) in corona discharge field, $E = 2.75 \cdot 10^6$ V/m and $\nabla E = 11 \cdot 10^8$ V/m^2; 3) capillary mouth in field; 4) in field, $E = -2.2 \cdot 10^6$ V/m and $\nabla E = -9.3 \cdot 10^8$ V/m^2; b) diagram of capillary placement in field. x^2, cm^2; τ, h.

did not differ significantly from those described in [3]. The discharge was created by a needle-plane electrode system.

The field intensity E of the discharge was measured in the evaporation zone by the probe body method from the amount of charge acquired by a spherical isolated probe at the point of the discharge studied [4]. A diagram of the measurement system is shown in Fig. 1a. The corona-producing needle electrode 1 is connected to the positive terminal of the high-voltage supply, and plane electrode 2 is grounded. Distance between electrodes in various experiments varied within the range $l = (4\text{-}10)$ cm. Test body 3 (metallic sphere with diameter $2a = 0.19$ cm) was suspended on a capron filament 4, 21 μm in diameter. The resistivity of this filament was $5 \cdot 10^{15}$ Ω·m. The length of the suspension filament $L = 0.4$ m was chosen so that the sphere lay coaxial with electrode 1 during measurements. After continuous increase of the voltage on the corona electrode to a specified value, the probe body and filament became charged and deviated from a vertical position. The final position of the sphere corresponded to the point at which field intensity was measured. The voltage was then continuously reduced to zero.

The charge of the test body was measured by its deviation in a homogeneous electric field of intensity E_0, created by plane capacitor 5. The probe body was moved into the capacitor by moving suspension arm 6 along guides 7. Inclination of the probe was determined by an optical system consisting of an objective lens and eyepiece-micrometer. To eliminate the charge of the filament from the calculations the sphere was discharged, after which its inclination in the homogeneous field was redetermined. The corona field intensity was calculated with the expression [4]

$$E = \frac{P(\Delta y_1 - \Delta y_2)}{12\pi\varepsilon_0 E_0 L a^2}. \quad (1)$$

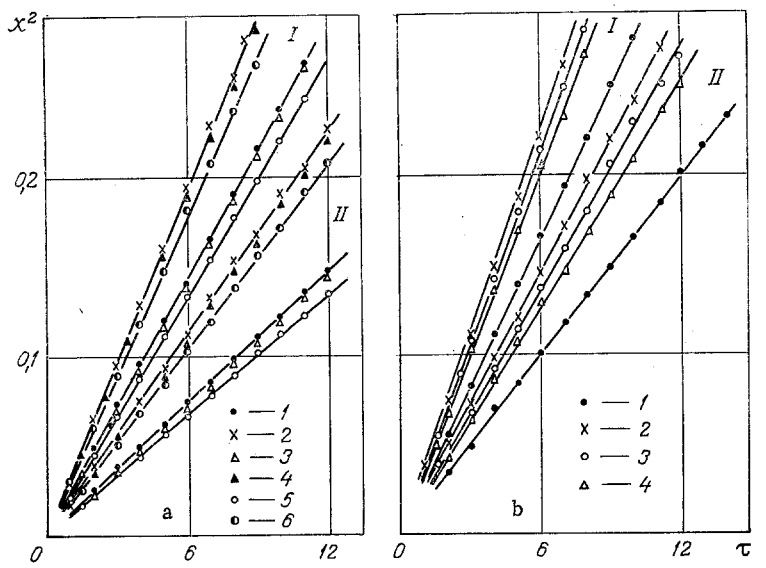

Fig. 3. $x^2(\tau)$ for evaporation of water (1, 2) and aqueous KCl solutions at C = 0.75% (3, 4), C = 7.5% (5, 6) from capillaries with r = 12.5 μm with corona discharge field applied, $E = 2.6 \cdot 10^6$ V/m and $\nabla E = 9.7 \cdot 10^8$ V/m² (2, 4, 6), and without field (1, 3, 5). (T = 296.5°K, $\varphi = 0.42$ (curves I), 0.71 (II) (a)); effect of air flow on water evaporation rate from capillaries with r = 10.4 μm at T = 297.2°K, $\varphi = 0.34$ (curves I), 0.60 (curves II): 1) measurements without field; 2) in field, $E = 2.7 \cdot 10^6$ V/m and $\nabla E = 9.9 \cdot 10^8$ V/m²; 3, 4) same values with $v_{air} = 0.9$ m/sec and $v_{air} = 1.5$ m/sec, respectively (b).

The mean value of E at the point was determined from the result of four to seven measurements. Relative uncertainty in field determination did not exceed 8%. The experimental E distribution along the capillary axis at $l = 5.2$ cm is shown in Fig. 1b. The same figure shows the theoretical value of E (curve 2), calculated with the method described in [5]. The length l is measured from the tip of the needle.

Observations were simultaneously performed on two capillaries with identical radii. The sealed liquid-filled capillary to be studied in the field was located on the same vertical axis as the needle electrode. A control capillary was placed outside the field in the same vertical plane as the test capillary. After placement in the chamber maintaining constant φ and T, the tops of the capillaries were cut off. This moment was chosen as the origin for time measurements ($\tau = 0$). The distance from the needle electrode to the capillary tip comprised 0.4 cm.

The results of experimental studies of the effect of subdischarge inhomogeneous electric fields on the rate of water evaporation from capillaries, presented in [3], were found to be in agreement with a previously developed theory [6], according to which there is added to the diffusion flow of vapor molecules q_v in an inhomogeneous electric field of intensity E an additional flow q_e. The total flow is then equal to:

$$q = q_v + q_e = -D\frac{dc}{dx}\left[1 + \frac{p_e \nabla E c}{kT(-dc/dx)}\right] = -D_*\frac{dc}{dx}. \qquad (2)$$

Figures 2 and 3a show some of the experimental results obtained for evaporation into air of water and KCl solutions from thin capillaries with and without the corona discharge field at various φ values. As is evident from the curves, application of the field leads to a marked increase in evaporation of water and KCl solutions from the capillaries, the field having a large effect when φ values in the chamber are higher. At $\varphi = 0$ the effect of the field on the evaporation process is insignificant. The functions $x^2(\tau)$ for evaporation in the field, as in the absence of field, are linear, which agrees with the well-known equation [7]

TABLE 1. Reduction in Vapor Pressure above Capillary Mouth in Corona Discharge Field and Linear Evaporation Rates of Water without Field U and in Field U*

φ	φ_*	$\bar{\varphi}_*$	D, cm²/sec	D_*, cm²/sec	D_*/D	$U\cdot10^6$, cm²/sec	$U_*\cdot10^6$, cm²/sec	U_*/U	r, μm
0,34	0,21	0,23	0,259	0,267	1,03	7,80	10,2	1,31	5,5
0,58	0,46	0,42	0,256	0,269	1,05	4,95	7,09	1,43	12,2
0,75	0,60	0,54	0,254	0,275	1,08	3,03	4,85	1,59	19,6

$$x^2 = 2\mu p_s D(\varphi_M - \varphi)\tau/\rho RT. \quad (3)$$

The field's effect on liquid evaporation rate is apparently produced by the action of the following factors. Within the capillaries the field acts as an inhomogeneous field source, i.e., to the diffusion flow of vapor molecules q_v there is added an electroconvective flow q_e. Outside the capillary the field acts as a dryer, reducing the vapor pressure above the capillary mouth. This effect could be produced either by screening of the capillary in the corona discharge zone by excess space charge of high density [8], which is produced mainly in the region of the central force line [5], or by sorption of vapor molecules on nuclei (ions) produced in the corona discharge. The convective action of the field leads to intense mixing of the vapor—gas mixture, which improves vapor removal from the capillary mouth. Some role in the acceleration of evaporation may be played by the liberation of Lentz—Joulean heat in the discharge gap. In our experiments temperature shift of the vapor—gas mixture in the evaporation zone did not exceed 0.2°, which corresponds to possible φ oscillations by ±0.01 at 295-297°K.

It is evident from Fig. 2 that the field exerts its greatest effect in the case where the intensity gradient of the applied field in the evaporation segment $\nabla E > 0$, i.e., when the directions of the electroconvective and diffusion vapor flows coincide (capillary positioned at point 2). If the field is applied such that $\nabla E < 0$, it produces somewhat less effect on the evaporation process (point 4). In this case the electroconvective flow is directed opposite to the diffusion flow of vapor molecules, although the effect of φ reduction above the capillary mouth does dominate. By placing the capillary so that only the mouth was within the discharge field, while ∇E was insignificant in the evaporation segment (point 3), the acceleration of evaporation due to reduction of vapor pressure above the capillary mouth and convection under the influence of the gasdynamic jet was estimated (point 3). The increase in water evaporation rate due to this effect comprises 23% at φ = 0.34, 32% (φ = 0.58) and 44% (φ = 0.75).

The curves of $x^2(\tau)$ for water evaporation without field are, as usual, linear and pass through the origin. The values of the diffusion coefficient D were obtained from the slopes of these lines. By substituting the values of the effective diffusion coefficient D* calculated with Eq. (2) in Eq. (3), the graphs of $x^2(\tau)$ for water evaporation in the field can be used to find the effective vapor pressure above the capillary mouth φ_*.

The reduction in vapor pressure in the discharge zone was also studied using an industrial specimen of KSM-5 silica gel, which has a rigid pore structure. A sphere of the silica gel with diameter $2a$ = 0.21 cm was suspended in the zone of evaporation from the capillaries on a calibrated quartz spring. The change in the length of the spring was determined with a KM-6 cathetometer. The length of the suspension was regulated so that when the steady-state was achieved the center of the sphere was located at a point corresponding to the position of the capillary mouth. After determining the mass of the dry specimen, it was maintained in the chamber for 3 h to establish an equilibrium moisture content W for the given value of φ = const. Then the corona discharge field was turned on and the decreased mass of the wet specimen determined after establishment of equilibrium. Using the value of W_* obtained in the field, the desorption isotherms of KSM-5 silica gel $W(\varphi)$ [2] were then employed to calculate the changed value of $\bar{\varphi}_*$. The results obtained are presented in Table 1. Also shown there are experimental values of D, D*, the ratios D*/D, and linear water evaporation rates without field U and with field U_*. The calculations were performed for T = 297°K, $\nabla E = 11\cdot10^8$ V/m², $p_e = 6.2\cdot10^{-30}$ C·m.

As is evident from Table 1, the effective vapor pressures in the discharge as measured by the capillary method are in agreement with the data obtained from desorption isotherms.

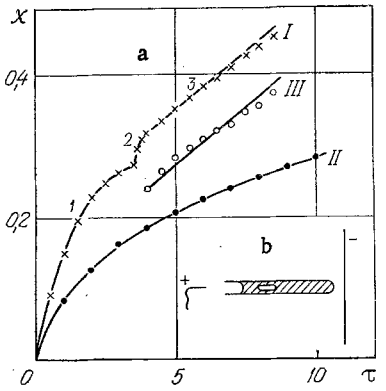

Fig. 4. Coordinate of main meniscus (I, II) and elongation of secondary water column (III) vs time (a): I, III) in discharge, $E = 2.7 \cdot 10^6$ V/m and $\nabla E = 12 \cdot 10^8$ V/m^2; II) without field ($\varphi = 0.80$, $r = 3.2$ μm, $T = 297.4°K$); 1) evaporation; 2) formation of secondary column; 3) flow of wetting film; b) diagram of capillary location relative to electrodes. x, cm.

Experimental values of the coefficient D are close to tabulated ones; the values of D_* agree satisfactorily with the data of [3] and the theory of [6]. The U_* values for given field parameters are larger, the higher the value of φ in the chamber.

It is evident from Fig. 3a that at concentrations $C \leq 0.75\%$ the curves for evaporation of KCl solutions and water practically coincide. For $C > 0.75\%$ in the absence of a field, the position of the $x^2(\tau)$ curves is in agreement with the data of [7]. Switch-on of the field leads to a significant increase in evaporation rate of the KCl solutions. At $\varphi = 0.42$, $E = 2.6 \cdot 10^6$ V/m, and $\nabla E = 9.7 \cdot 10^8$ V/m^2 the ratio U_*/U comprises 1.33 ($C = 0.75\%$) and 1.34 for $C = 7.5\%$. For the case of $\varphi = 0.71$ this value is equal to 1.52 for $C = 0.75\%$ and 1.54 for $C = 7.5\%$.

To determine the convective action of the discharge in evaporation from capillaries, a series of experiments was performed to study the effect of draft on the capillary by an external air current. Figure 3b shows some of the results obtained. These confirm the conclusion reached above as to reduction in relative humidity of the air in the discharge as compared to the surrounding medium. In fact, draft of the capillary by a flow of moister air leads to a higher reduction in evaporation rate, the greater the velocity of the draft. The external flow encourages equalization of the concentration of vapor molecules in the zone of evaporation from the capillaries, where the vapor pressure is reduced under the action of the field. An electrical wind may have a similar action [5, 8].

At high values of relative humidity in the chamber ($\varphi \geqslant 0.80$) after opening of the capillary and application of the field (capillary oriented with mouth toward needle electrode and in the same vertical line as electrode), for the first 3-4 h intense evaporation occurs (Fig. 4, curve I, 1). Then, in the capillary segment from which the liquid has evaporated, there appear secondary water columns 0.1-0.3 mm in length which confine air bubbles within the capillary. At distances from the capillary mouth to the liquid meniscus of $x \leq 0.4$ cm, bridges form predominantly at the mouth, while if the meniscus is further removed, the columnlets are formed no more than 3-4 mm from the meniscus.

Formation and growth of secondary columns in a corona discharge field (Fig. 4) can be explained by the fact that under the influence of the ponderomotive force [9]

$$P_e = (\varepsilon - 1)\nabla E^2/8\pi, \tag{4}$$

acting on a volume element of dielectric in an inhomogeneous electric field of intensity E, the effective thickness of the wetting film, which, as is well known [10, 11], is formed beyond the retreating meniscus, will be increased due to liquid supply from the main column. The dielectric liquid film is attracted by the field from the liquid volume beneath the meniscus and moves in the direction of increasing field inhomogeneity to the capillary mouth. We note that over 15-20 min before formation of the secondary columnlet, the rate of motion of the main meniscus of evaporating liquid down into the capillary increases greatly (curve I, 2). This thick film of liquid which forms on the capillary walls is obviously not in equilibrium. Developing thickness fluctuations cause it to flow together, forming bridges. Similar phenomena in nonequilibrium films were previously studied in [12].

After bubbles of vapor—gas mixture are formed, they move down into the liquid-filled capillary. This means that the water is pumped through the film between the menisci in the direction of greater field inhomogeneity closer to the capillary mouth. This effect leads to an abrupt increase in evaporation. Similar results were obtained in experiments with

ethylene glycol ($p_e = 7.4 \cdot 10^{-30}$ C·m) and butyl alcohol ($p_e = 5.5 \cdot 10^{-30}$ C·m). In addition, no effect was noticed when a corona discharge field ($E \leq 3 \cdot 10^6$ V/m and $\nabla E \leq 1.3 \cdot 10^8$ V/m^2) was applied during evaporation of nonpolar benzene ($p_e = 0$) in thin capillaries.

In evaporation of KCl solutions ($C \geqslant 0.075$ mass %) film flow along the capillary walls under the action of the discharge was not observed. This may be explained by suppression of the splitting pressure by ion-electrostatic forces in solutions of electrolytes, which leads to loss of film stability [13, 14]. Here the field exerts an effect on movement of the vapor only.

The results of the studies performed indicate that a corona field discharge has a significant effect on the mechanism and kinetics of internal mass transfer in capillaries, which are a model of porous structures. For $\varphi < 0.8$ use of such a field can lead to an increase in liquid evaporation rate from the capillaries by a factor of 1.5-2 times, mainly due to reduction of φ near the capillary mouth. At higher values of φ the water evaporation rate increases 3-5 times. This effect is achieved due to flow of liquid to the capillary mouth along the thick film which is pulled by the inhomogeneous electric field along the capillary walls. The data obtained show that the inhomogeneous electric field of a corona discharge can be used to intensify dehydration, capillary saturation, and drying of dispersed materials, significantly reducing the time required for these processes. This leads to a reduction in energy expenditure and increased efficiency of the technological process.

NOTATION

$\varphi = p/p_s$; p, water vapor pressure; p_s, pressure of saturated vapor; x, distance from liquid meniscus to capillary mouth; E, intensity of corona discharge field; E_o, intensity of electric field produced by planar capacitor; P, weight of probe body; Δy_1, deviation of center of charged sphere from vertical with horizontal field component E_o; Δy_2, sphere deviation from vertical after discharge; ε_o, ε, dielectric permeativities of vacuum and liquid; D, vapor diffusion coefficient through air; D_*, effective diffusion coefficient; dc/dx, vapor molecule concentration gradient; p_e, molecular dipole moment; k, Boltzmann's constant; T, temperature; μ, mass of mole of water; φ_M, relative vapor pressure above meniscus; ρ, density of water; R, ideal gas constant; φ_*, φ_*, effective relative vapor pressure in discharge, as measured by capillary method and desorption isotherms, respectively; V_{air}, velocity of air draft.

LITERATURE CITED

1. M. S. Panchenko, A. L. Panasyuk, I. N. Karpovich, and N. Ya. Kisel'chuk, "Kinetics of drying a capillary-porous body in an electric field," Inzh.-Fiz. Zh., 33, No. 2, 356-357 (1977).
2. M. S. Panchenko, A. S. Mosievich, A. L. Panasyuk, and I. N. Karpovich, "Effect of electrical and magnetic fields on pore space geometry and sorption capacity of dispersed bodies," Elektron. Obrab. Mater., No. 6, 40-44 (1976).
3. I. N. Karpovich, N. V. Churaev, and M. S. Panchenko, "Effect of inhomogeneous electric field on water evaporation from capillaries," Kolloidn. Zh., 42, No. 4, 634-638 (1980).
4. V. A. Babashkin and I. P. Vereshchagin, "Measurement of corona discharge field intensity by the probe body method," in: High Electric Fields in Technological Processes [in Russian], Moscow (1971), No. 2, pp. 3-11.
5. V. I. Levitov (ed.), Electrical Smoke Filters [in Russian], Énergiya, Moscow (1980).
6. A. L. Panasyuk, M. S. Panchenko, V. M. Starov, and N. V. Churaev, "Effect of an inhomogeneous electrical and magnetic field on internal mass transfer in capillary-porous bodies," Inzh.-Fiz. Zh., 35, No. 1, 93-100 (1978).
7. R. A. Tishkova, N. V. Churaev, and A. P. Ershov, "Evaporation rates of concentrated electrolyte solutions from thin capillaries," Inzh.-Fiz. Zh., 37, No. 7, 849-853 (1979).
8. N. S. Kaptsov, The Corona Discharge [in Russian], Gostekhizdat, Moscow—Leningrad (1947).
9. I. E. Tamm, Fundamentals of the Theory of Electricity [in Russian], Nauka, Moscow (1976), p. 148.
10. B. V. Deryagin, N. V. Churaev, and I. G. Ershova, "Flow in surface layers in water evaporation from capillaries," Dokl. Akad. Nauk SSSR, 182, No. 2, 368-371 (1968).
11. N. V. Churaev and I. G. Ershova, "Anomolous behavior of polar liquids in evaporation from quartz capillaries," Kolloidn. Zh., 33, No. 5, 771-777 (1971).

12. N. V. Berdinskaya and M. M. Kusakov, "Experimental study of the mechanism of liquid transfer from the film to capillary-contained state in the capillary pore model," Kolloidn. Zh., 34, No. 5, 755-760 (1972).
13. B. V. Deryagin and M. M. Kusakov, "Experimental study of solvate surfaces," Izv. Akad. Nauk SSSR, Ser. Khim., No. 5, 1119-1122 (1937).
14. B. V. Deryagin and S. V. Nerpin, "Equilibrium, stability, and kinetics of free liquid films," Dokl. Akad. Nauk SSSR, 99, No. 6, 1029-1032 (1954).

COLLECTIVE EFFECTS IN A DENSE SYSTEM OF LARGE BUBBLES

Yu. A. Buevich

UDC 532.529

The rising velocity and interphase transport of a dense bubble swarm in a homogeneous liquid are investigated, along with the motion and external mass transfer in an inhomogeneous porous medium.

Under confined-flow conditions the interaction of bubbles forming a dense swarm significantly alters their hydrodynamic and mass-transfer characteristics in comparison with solitary bubbles. The values of the Reynolds number, which characterizes the flow around solitary bubbles, are usually large in the majority of real situations, so that the liquid flow in the space between bubbles can be regarded as inviscid and potential everywhere except in thin boundary layers on the bubble surfaces and in their hydrodynamic wake regions. In this article we investigate the two extreme cases in which the influence of surface tension is very strong and very weak and, accordingly, the bubbles approach the configurations of a sphere and a spherical cap.

The motion of solitary bubbles of the first type was first studied theoretically in [1, 2], and their mass transfer with the surrounding medium in [3]. A hydrodynamic model of bubbles of the second type was first proposed by Davies and Taylor [4] and was later refined by Parlange [5]; their mass transfer with the surrounding medium has been investigated in [6, 7], and bubbles of this type have been investigated more in detail in [8, 9]. Collective effects have apparently been studied only for spherical bubbles on the basis of the well-known cell model [10, 11]. Below, we investigate these effects by means of the powerful machinery of ensemble averaging and the methods of self-consistent field theory (see [12] and the survey [13]).

Filtration and External Mass Transfer in an Inhomogeneous Porous Solid

We first consider the auxiliary problem of determining the effective permeability of an inhomogeneous porous solid comprising a macroscopically homogeneous porous medium ("matrix") and discrete porous inclusions, which are also macroscopically homogeneous and are distributed in the matrix. The Darcy equations

$$\mathbf{Q}_i = -(k_i/\mu)\nabla P_i, \quad \operatorname{div}\mathbf{Q}_i = 0 \tag{1}$$

for the local values of the filtration rate Q and the pressure P are valid in the matrix and in the inclusions. At the boundaries of the inclusions the pressure and the normal component of the flow velocity are continuous. It is required to determine the "effective" permeability k, i.e., the coefficient in the equation $\mathbf{q} = -(k/\mu)\nabla p$, which relates the mean filtration rate to the pressure in the inhomogeneous solid (in the simplest case q and p can be interpreted as the results of averaging Q and P over a "small" physical volume containing a sufficiently large number of inclusions).

The statement of this problem is identical to the statement of the problem of determining the effective thermal conductivity of a composite material if the pressure is identified

Ural State University, Sverdlovsk. Translated from Inzhenerno-Fizicheskii Zhurnal, Vol. 41, No. 6, pp. 1057-1066, December, 1981. Original article submitted November 30, 1980.

0022-0841/81/4106-1339$07.50